Geomorphology 336 (2019) 18–30

Contents lists available at ScienceDirect

Geomorphology

journal homepage: www.elsevier.com/locate/geomorph

Evolution of fluviokarst canyons in response to the Quaternary tectonic uplift of the Apulia Carbonate Platform (southern Italy): Insights from morphometric analysis of drainage basins

Mariantonietta Donnaloia [a,*], Emanuele Giachetta [b,c], Domenico Capolongo [a], Luigi Pennetta [a]

[a] Dipartimento di Scienze della Terra e Geoambientali, Università degli Studi di Bari "Aldo Moro", via Orabona 4, 70125 Bari, Italy
[b] Istituto per il Rilevamento Elettromagnetico dell'Ambiente (IREA), Consiglio Nazionale delle Ricerche, via Giovanni Amendola, 122/D, 70126 Bari, Italy
[c] ETH Swiss Federal Institute of Technology, Geological Institute, Sonneggstrasse 5, 8092 Zürich, Switzerland

ARTICLE INFO

Article history:
Received 22 October 2018
Received in revised form 5 March 2019
Accepted 5 March 2019
Available online 11 March 2019

Keywords:
Fluviokarst drainage basins
Drainage reorganization
Murge Plateau uplift
Quaternary landscape evolution

ABSTRACT

The evolution of fluviokarst landscapes results from the interplay of karst and fluvial processes, all driven by rock uplift or base level fall. The fluviokarst landscape of the Murge Plateau in the central Apulian Region (southeastern Italy) is characterized by narrow, steep-sided, V-shaped canyons, locally called 'Gravine', and deeply incised into the Plio-Pleistocene deposits of the Bradanic Trough and the underlying Apulian limestone bedrock. Previous studies propose alternative models of canyons development, however identifying a dominant morphogenetic process for the evolution of the 'Gravine' fluviokarst drainage basins remains an open question. The results of our regional morphometric analysis reveal a marked transition from the relict, low-relief landscape preserved in the Murge uplands to the steep channel reaches below prominent knickpoints showing evidence of a transient wave of river incision that is propagating inland. We observe anomalies of mean local relief and channel steepness, and the distribution of fluvial knickpoints consistent with a regional uplift affecting the Murge Plateau since Middle-Late Pleistocene. These findings demonstrate that the history of landscape evolution was dominated by fluvial processes. Using transformed river profile analysis we show that χ anomalies in the 'Gravine' trunk channels indicate drainage basin instability by drainage area capture. The convex-shape of the hypsometric curves and high hypsometric integrals confirm that the disequilibrium state of the 13 analyzed basins results from a combination of regional uplift and subsequent river network reorganization and plateau area captures. Based on our results, we propose a new model of landscape evolution for the 'Gravine' fluviokarst drainage basins.

1. Introduction

The Murge Plateau in the central Apulian Region (southeastern Italy) is a low-relief landscape, entirely underlain by Mesozoic carbonate rocks, thereby characterized by distinctive karst morphological features, such as dolines, cave systems, and poljies that indicate prolonged dissolution (Moresi and Mongelli, 1988; Delle Rose and Parise, 2002; Parise, 2006). However, fluviokarst canyons (locally called 'Gravine') developed along the southwestern margin of the Murge Plateau (Boenzi, 1954; Tropeano, 1992; Mastronuzzi and Sansò, 1993; Parise, 2007), where the remains of siliciclastic regressive deposits of the Bradanic foredeep are superimposed on the limestone bedrock (Mongelli and Ricchetti, 1970; Ricchetti, 1980; Casnedi, 1988). The sharp morphological differences between the inner Murge Plateau and the impressive, up to 200 m deep fluviokarst canyons flowing to the southwest, suggest a transient response of the fluviokarst landscape caused by a change in the rate of either rock uplift or base-level fall (e.g., Bishop et al., 2005; Berlin and Anderson, 2007; Kirby and Whipple, 2012; Whittaker, 2012; Scotti et al., 2014).

River networks preserve a record of the history of landscape evolution because continuous interplay between tectonics, climate and earth surface processes sets the relief and shape of drainage basins (Whipple and Tucker, 1999; Willett et al., 2014; Giachetta and Willett, 2018a). One method of interpreting fluvial landscapes and investigating the factors influencing river incision is the analysis of longitudinal river profiles (Snyder et al., 2000; Wobus et al., 2006; Perron and Royden, 2013). River profiles with a smooth, concave-upward longitudinal profile are the expression of equilibrium between erosion, rock uplift, and climate (Gilbert, 1877; Mackin, 1948; Leopold and Maddock, 1953). Deviations from the graded shape of river profiles indicate disequilibrium produced by recent changes of factors controlling landscape denudation (Tucker and Slingerland, 1997; Whipple and Tucker, 1999). In fluviokarst landscapes, the interpretation of river profiles is potentially impacted by other factors governing the evolution of channel networks, such as the relative influence of dissolution and

* Corresponding author.
E-mail address: mariantonietta.donnaloia@uniba.it (M. Donnaloia).

https://doi.org/10.1016/j.geomorph.2019.03.008
0169-555X/

mechanical processes on the erosion of the river bed, diversion of surface flow to the subsurface karst systems, and groundwater sapping (e.g., Dunne, 1980, 1990; Schorghofer et al., 2004; Anthony and Granger, 2007; Woodside et al., 2015; Francis et al., 2018). Furthermore, repeated transitions from a prevalence of dissolution processes to dominant fluvial erosion can result in hybrid or transitional landforms and complex patterns of erosion that render the interpretation of the fluviokarst landscape in terms of climate or uplift change problematic (Gallen and Wegmann, 2017; Phillips, 2017, 2018).

A few studies explored the formation and evolution of the 'Gravine' canyons in the Murge Plateau, although the relation between tectonics and erosion as well as the relative dominance of fluvial and karst processes is still controversial. It was argued that the regional tectonic uplift has affected this area since the Middle-Upper Pleistocene creating preferential water flow pathways and encouraged the development of karst processes along discontinuities (Beneduce et al., 2004), which progressively affected the limestone bedrock. Hence, in addition to the physical erosion exerted by concentrated water flow, the morphological evolution of these landforms was subordinately linked to limestone dissolution (Mannella, 1977). Chemical weathering of the limestones bedrock caused widening of fractures, thereby favoring mechanical erosion and deep incision of the 'Gravine' canyons (Beneduce et al., 2004). Conversely, Boenzi et al. (1976) proposed that the 'Gravine' valleys have a fluvial origin, arguing that an antecedent drainage network formed over the siliciclastic units and thus, it was superimposed by the progressive incision of the canyons into the underlying carbonate rocks. Mastronuzzi and Sansò (2002) argued that groundwater sapping was the main process involved in the development of the fluviokarst canyons in the southwestern Murge Plateau. The authors proposed that the almost flat morphology of the Murge Plateau, the calcareous nature and high permeability of its terrains concentrated groundwater sapping and retrogressive incision in the channel heads of the 'Gravine' canyons (Kirkby and Chorley, 1967; Dunne, 1980; Mastronuzzi and Sansò, 2002).

In this study, we perform a morphometric analysis at the regional-to-catchment scale to investigate the Quaternary landscape evolution of the western Murge Plateau. We examine the regional tectonic signal and the geomorphic response by calculating morphometric parameters from a Digital Elevation Model (DEM) at 90 m resolution. We investigate the state of equilibrium of the 'Gravine' by analyzing morphometric indexes of 13 catchments and identify anomalies in the trunk channels from longitudinal and transformed river profiles. Our main goals are to characterize the transient state of these fluviokarst drainage basins that was produced by the Quaternary uplift of the Apulian foreland and to determine whether fluvial processes dominated in the subsequent development of the 'Gravine'. Based on our results and observations, we develop a conceptual model of Quaternary landscape evolution for the western Murge Plateau.

2. Geological and geomorphological settings

The Murge Plateau is located in the central Apulia Region and represents the foreland of the Southern Apennines fold-and-thrust belt that developed by the convergence between the African and Eurasian plates during the Cenozoic (Dewey et al., 1989; Billi, 2005). The Murge Plateau consists of a 6 km thick sequence of shallow marine limestones and dolomites of the Calcare di Bari and Calcare di Altamura Mesozoic lithostratigraphic formations (D'Argenio, 1974) that were flexurally exposed and karstified since the Late Cretaceous (Tropeano and Sabato, 2000; Tropeano et al., 2002). Starting from the Late Pliocene-Early Pleistocene, a wide area of the western Apulian carbonate platform underwent tectonic subsidence associated to the east-southeastward migration of the Southern Apennines belt and the simultaneous development of the Bradanic Trough, a flexural depression at the front of the thrust belt (Iannone and Pieri, 1982; Patacca and Scandone, 2001; Tropeano et al., 2002). During the initial phase of flexural subsidence, the Apulian carbonate bedrock was covered by the accumulation of foredeep sediments consisting mainly of turbidites, followed by the deposition of Upper Pliocene to Quaternary sediments, consisting of hemipelagic silty clay, and finally, coarse-grained, shallow-marine siliciclastic and carbonate sediments of the last regressive cycle (Valduga, 1973; Ciaranfi et al., 1979).

The regional tectonic trend changed since Middle-Late Pleistocene times, when the whole area underwent regional uplift that resulted in about a 1 km flexural bulge of the Apulia foreland (Billi and Salvini, 2003), coeval uplift of the Bradanic foredeep deposits up to 500–600 m, and deposition of a staircase of marine terraces along the Ionian coast (Tropeano et al., 2002). Ferranti et al. (2006) estimated the vertical displacement rates affecting the Central Mediterranean since the Last Interglacial sea level highstand (MIS 5.5) based on the relative altitude distribution of geomorphological markers, such as marine terraces, notches, and other biological indicators. The estimated Quaternary uplift rates varied from a maximum of 0.25 mm/yr along the Ionian coast, to 0–0.02 mm/yr along the Adriatic coast (Ferranti et al., 2006).

Differential rates of flexural retreat across adjacent segments resulted in the transverse accommodation faults and the fragmentation of the present Apulian forebulge into three structural domains (Royden et al., 1987; Favali et al., 1993; Mariotti and Doglioni, 2000; Billi, 2005): the Gargano Promontory located in the northern part of Apulia, the Murge Plateau in the central part, and the Salento Peninsula in the southern part (Fig. 1a). The Murge Plateau is separated from the Gargano Promontory by the Ofanto Graben, and from the Salento Peninsula by an escarpment called Soglia Messapica (Pieri et al., 1997; Festa et al., 2018).

The main landscape components of the study area are: (1) the low-relief top surface of the Murge karst Plateau that is almost entirely underlain by Mesozoic carbonate rocks; (2) the southwestern escarpment of the Murge plateau, where the contact between the Plio-Pleistocene siliciclastic deposits and the underlying Mesozoic carbonates is exposed; and (3) the eastern margin of the Bradanic Trough, extending along the Ionian coastal plain that is underlain by Quaternary marine and continental terrace deposits (Fig. 1b).

The Murge Plateau corresponds to a morpho-structural high in the Apulian carbonate platform forming a wide antiformal structure. The Higher Murge Plateau is the inner portion of the plateau that reaches the higher elevations, while the Lower Murge Plateau is the portion of the plateau with progressively lower elevations toward the Adriatic Sea. Large-scale karst landforms, such as dolines and caves are mostly found in the Higher Murge Plateau (Parise, 2003; Parise, 2006). The karstification of the Murge Plateau is related to the recurring phases of subaerial exposure of the Apulian Mesozoic carbonates since the Upper Cretaceous. Consequently, most karst areas of the Murge Plateau are extensively covered by 'Terra rossa', a clay-rich residual soil resulting from the dissolution of the underlying carbonates (Moresi and Mongelli, 1988), that can locally be up to 10 m thick in morphological depressions (Spalluto and Caffau, 2010).

The landscape of the western Murge Plateau is characterized by the canyons of the 'Gravine' fluviokarst drainage basins that developed along a prominent, southwest-facing plateau escarpment. The 'Gravine' are ephemeral streams with low discharge for most of the year, but during heavy rainfall events they have a torrential flow regime associated with episodic fluvial erosion. The relatively impermeable top layer consisting of Plio-Pleistocene clays and 'Terra rossa' residual soils in the upper 'Gravine' catchments could significantly contribute to increase surface runoff on the Murge Plateau, and cause the frequent floods reported in the 'Gravine' streams by historical data (e.g., Manfreda et al., 2015, and references therein). Several 'Gravine' streams are allogenic streams sourcing in adjacent clastic rocks of the Bradanic Trough, rather than deriving their streamflow from the karst areas.

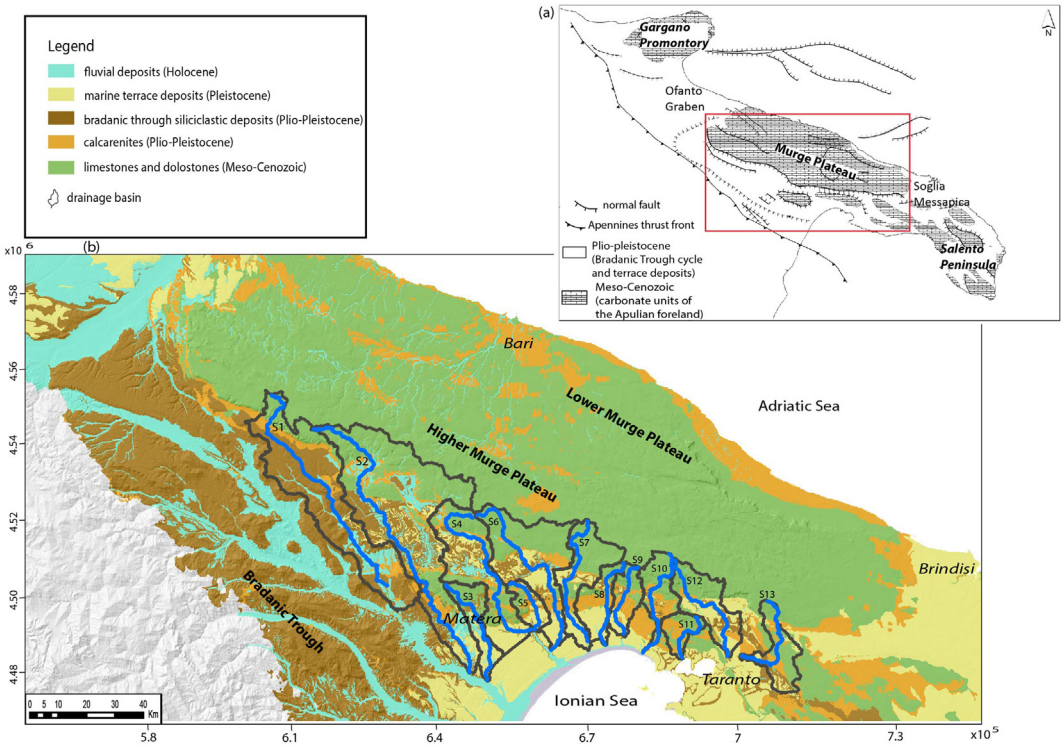

Fig. 1. a) Schematic structural map of the Apulia region (modified from Pieri et al., 1997); b) geological sketch of the study area, draped over shaded relief. Analyzed streams are displayed (S1 = Torrente Gravina stream, S2 = Gravina di Matera stream, S3 = Gravina di Ginosa stream, S4 = Gravina di Laterza stream, S5 = Gravina di Montecamplo stream, S6 = Gravina di Castellaneta stream, S7 = Gravina di Palagianello stream, S8 = Gravina Capo di Gavito stream, S9 = Gravina Monte S. Elia stream, S10 = Gravina di Leucaspide stream, S11 = Gravina di Mazzaracchio stream, S12 = Canale Visciolo stream, S13 = Gravina di Villa Castelli stream).

The 'Gravine' canyons are narrow, steep-sided, V-shaped valleys deeply incised into Plio-Pleistocene deposits and underlying limestone bedrock (Fig. 2a). The canyon flanks display a gentler slope where the Plio-Pleistocene calcarenites deposited on top of the Mesozoic limestones exist. The flanks of the 'Gravine' streams are locally affected by hillslope instability that is favored by the presence of intense rock fracturing and karst cavities (Fig. 2b). Most of the channels consist of limestone bedrock covered by a patchy veneer of limestone gravels. Limestone blocks are supplied locally by the steep valley sides and transported downstream during extreme flood events (Fig. 2c). Plucking of rock particles from the river bed is frequently observed along the channels (Fig. 2d).

The stepped surface morphology corresponding to a flight of Pleistocene marine terraces characterizes the landscape below the

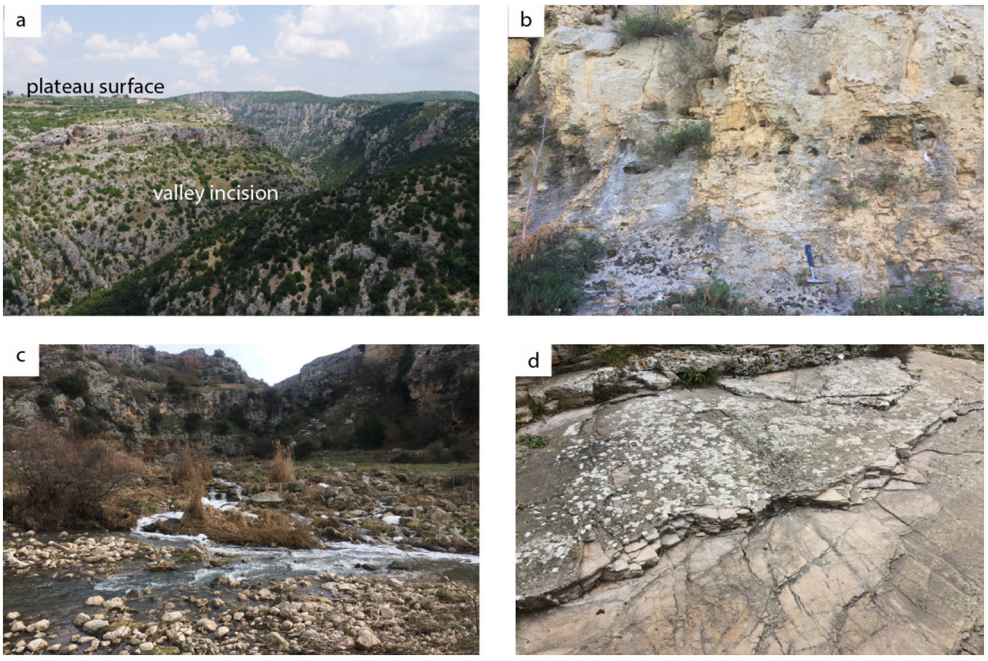

Fig. 2. Gravina di Matera: a) aerial view of the sub-horizontal plateau surface and the valley incision, b) karst cavities c) subrounded to angular pebbles and cobbles along the Gravine stream bed and d) plucking along strata.

western Murge Plateau. Along the southwestern Apulian margin, raised marine platforms were cut into the limestone bedrock and the overlying sediments of the Bradanic Trough, and are found at elevations up to 400 m above sea level (Mastronuzzi and Sansò, 2002). The oldest terrace is deeply incised by the 'Gravina Gennarini' and 'Gravina di Leucaspide' streams and is 300 ky old (Dai Pra and Steams, 1977; Mastronuzzi and Sansò, 2002). The Pleistocene marine deposits stretch 200 km along the Ionian coast and their elevation decreases from north to south, indicating regional tilting (Dai Pra and Hearty, 1988; Bordoni and Valensise, 1998; Cucci and Cinti, 1998; Amato, 2000; Ferranti et al., 2006).

3. Methods

3.1. Swath profiles and local relief

The analysis of topographic swath profiles was used to perform a large-scale analysis of relief and to characterize the spatial pattern of tectonic deformation across the Apulian foreland (Isacks, 1992; Fielding et al., 1994; Grohmann, 2004; Telbisz et al., 2013). We extracted three topographic swath profiles from the Shuttle Radar Topography Mission (SRTM) 90 m resolution DEM, using the 'swath' function implemented in the Topotoolbox version 2.0.1 for the MATLAB software (Schwanghart and Scherler, 2014). Two of these profiles cross the Murge Plateau at its largest width and one at its largest length. We subdivided each profile into a series of parallel, 5 km long and 500 m wide, rectangular swaths centered on each profile. The swath profile was obtained by projecting the elevation data from each rectangular swath onto a vertical plane and calculating the mean, maximum, and minimum elevations. We generated a map of mean local relief (Ahnert, 1970; Gilchrist et al., 1994; Hurtrez et al., 1999; Kühni and Pfiffner, 2001; Montgomery and Brandon, 2002) of the study area to explore the spatial distribution of landscape dissection by streams and highlight differences in geomorphic response across the Murge Plateau landscape. We extracted the maximum and minimum elevation grids from the original DEM by using the "localtopography" Topotoolbox function (Schwanghart and Scherler, 2014) and a circular moving window with a radius of 1 km, which is the average distance between the major Gravine valleys in the western Murge Plateau. The local relief map was obtained by subtracting the minimum elevation grid from the maximum elevation grid.

3.2. Morphometric analysis of drainage basins

We performed a morphometric analysis at a basin scale to investigate the landscape response to the Quaternary regional uplift. All morphometric parameters were determined from the 90 m resolution SRTM DEM using GIS-based techniques implemented in the Topotoolbox version 2.0.1 (Schwanghart and Scherler, 2014).

The Hack's law, is an empirical scaling relationship between channel length, L, and drainage area, A (Hack, 1957):

$$L = c \cdot A^h, \tag{1}$$

where c is a dimensional coefficient that varies among basins [L^{2-h}] and h is a dimensionless constant that was found to be 0.5–0.6 for a variety of basin areas (Hack, 1957; Gray, 1961; Leopold et al., 1964; Mueller, 1972). We performed a linear regression in a log distance - log area graph calculating the Hack's index, h, and the coefficient c, to characterize river networks in our fluviokarst drainage basins.

To investigate the relations between relief, uplift, and denudation in the selected catchments, we calculated the mean local relief (*mlr*), its standard deviation, and the total relief (*tbr*) (Ahnert, 1970; Frankel and Pazzaglia, 2005). To investigate the state of equilibrium between uplift and erosion processes, we calculated the basin hypsometric curve and the Hypsometric Integral (*HI* index) (Strahler, 1952). The shape of hypsometric curves provides evidence of the basin evolutionary stage and highlights local effects of erosion and tectonic uplift (Strahler, 1952). S-shaped or almost straight hypsometric curves indicate near-equilibrium and actively eroding landscape; a convex shape of the hypsometric curve suggests instability due to base level fall. Concave hypsometric curves are typical of basins dominated by fluvial incision in tectonically stable landscapes. The *HI* index varies between 0 and 1: high *HI* values can be related to disequilibrium between uplift and erosion produced by recent tectonic activity, whereas low *HI* could indicate that fluvial activity dominates erosion processes in tectonically stable catchments (Strahler, 1952; Willgoose and Hancock, 1998; Hurtrez et al., 1999).

3.3. River profile and χ-plot analysis

The elevation of longitudinal river profiles is controlled by the interplay between uplift rate, U, and erosion rate, E, and the rate of elevation change at a location x along the channel and at time t is described by Whipple and Tucker (1999):

$$\frac{\partial z}{\partial t} = U(x,t) - E(x,t), \tag{2}$$

where the erosion term E is often modelled using the stream-power law (Howard and Kerby, 1983; Howard, 1994; Whipple and Tucker, 1999) that relates channel incision into bedrock to upstream drainage area, A, and channel slope, S:

$$E = KA^m S^n, \tag{3}$$

Here, K is bedrock erodibility, and m and n are positive dimensionless constants (Whipple and Tucker, 2002). A perfect slope-area scaling is expected for steady-state river profiles form Eqs. (1) and (2) (Hack, 1957):

$$S = k_s A^{-\theta}, \tag{4}$$

where the channel steepness k_s is a function of rock uplift and bedrock erodibility, and $\theta = m/n$ is the channel concavity (Flint, 1974). This scaling is empirical, but is consistent with a wide range of incision laws. Equilibrium river profiles typically exhibit a concavity index of 0.35–0.6 (Whipple and Tucker, 1999).

Digital elevation models can be used to extract information about uplift and stream-power parameters (θ and k_s indexes) from regression on log-log plots of slope and drainage area data (Wobus et al., 2006), although this methodology has some relevant disadvantages. A significant limitation of the slope-area analysis is that taking the derivative of already noisy elevation data enhances unwanted data scatter in slope–area plots, reducing the accuracy of identified power-law trends (Perron and Royden, 2013).

Recently, a method has been developed for the analysis of longitudinal stream profiles that is based on the integral form of the steady-state river profile that is obtained by integrating both sides of Eq. (4) with respect to distance:

$$z(x) = z(x_b) + k_s \int_{x_b}^{x} \frac{dx}{A(x)^\theta}, \tag{5}$$

where z is elevation and $z(x_b)$ is the elevation at a base level. For the simple case of uniform U and K, Eq. (5) can be simplified to (Giachetta and Willett, 2018a):

$$z(x) = z(x_b) + {A_o}^{-m} k_s \chi, \tag{6}$$

The quantity χ is an integral function of position along the channel network and has dimensions of length:

$$\chi = \int_{x_b}^{x} \left(\frac{A_o}{A(x)} \right)^{\theta}, \quad (7)$$

where A_0 is an arbitrary scaling area. When a value of $A_0 = 1$ is used, k_s is simply the slope of the elevation against χ plot (Yang et al., 2015). The integral form of the stream power model in Eq. (6) predicts that equilibrium river profiles will be identified by a straight line (Perron and Royden, 2013). To analyze the state of equilibrium of the studied basins, we calculated the χ-plots of channel networks and determined the best-fit concavity and steepness indexes for each basin by regression analysis (Perron and Royden, 2013). We performed a linear least-squares regression through χ-elevation data of each basin and obtained the best-fit value of m/n producing the highest R^2.

We performed a river profile analysis using the integral approach implemented in the TopoToolbox v. 2.0.1 (Schwanghart and Kuhn, 2010; Schwanghart and Scherler, 2014). After DEM filling, a flow direction grid was obtained by using the 'FLOWobj' TopoTollbox function. The stream network was determined by calculating the flow accumulation grids using the 'flowacc' Topotoolbox function and a threshold area of 10^6 m^2 for channel head initiation (Montgomery and Foufoula-Georgiou, 1993; Wobus et al., 2006). We delineated 13 drainage basins from the flow-direction grid and extracted the main stem from each basin (Fig. 1). We calculated the χ-plot for the river network of each drainage basin using the 'chiplot' Topotoolbox function (Schwanghart and Scherler, 2014), which performs a linear regression analysis through χ-elevation data to find the best-fit basin concavity (Eq. (7); Perron and Royden, 2013).

The steepness index, k_s, is sensitive to spatial variations of lithology, climate and rock uplift, and it covaries with the concavity index, θ. Thus, to compare the steepness indexes from drainage basins with different best-fit concavities, we constructed the χ-plots of trunk channels using a reference concavity $\theta_{ref} = 0.45$, and derived values of normalized steepness index, k_{sn} (Wobus et al., 2006; Kirby and Whipple, 2012). We identified linear channel reaches along the χ-plot of each trunk channel and determined their k_{sn} value as the slope of the regression line (Gallen and Wegmann, 2017; Fig. 7). For each basin, we constructed the χ-plot of the trunk using a scaling area of $A_0 = 1$ m^2, and a reference river concavity $\theta_{ref} = 0.45$ (Eq. (7)). For each trunk, we identified linear channel segments bounded by significant slope breaks in the linear scaling between χ and elevation data (knickpoints). We performed linear regression through each linear χ-plot segment to quantify the normalized channel steepness index k_{sn} (Gallen and Wegmann, 2017).

We used 1:100 000 geologic maps from the Servizio Geologico d'Italia: 'Foglio 188' (Azzaroli et al., 1968a, 1968b), 'Foglio 189' (Azzaroli et al., 1968a, 1968b), 'Foglio 190' (Merla and Ercoli, 1971), 'Foglio 200' (Boenzi et al., 1971a, 1971b), 'Foglio 201' (Boenzi et al., 1971a, 1971b) and 'Foglio 202' (Martinis and Robba, 1971) as working base to identify rock type changes and tectonic features along each river. The main lithologies cropping out in the selected basins were digitized (Fig. 1) and classified as: Meso-Cenozoic carbonate units of the Apulian foreland (limestones and dolostones); Plio-Pleistocene calcarenites; Plio-Pleistocene clays, sandstones, and conglomerates of the Bradanic Trough regressive cycle; Pleistocene marine terrace deposits; and Holocene fluvial terraces and alluvial deposits. To determine whether the spatial changes of channel steepness correlate with lithology, we used Eq. (4) and a reference concavity $\theta_{ref} = 0.45$ to derive a map of the normalized channel steepness index, k_{sn}, from the DEM (Wobus et al., 2006).

4. Results

4.1. Swath profiles and local relief analysis

The Murge Plateau consists of a karstic ridge elongated in the NW-SE direction (Fig. 3A and B), corresponding to the forebulge of the Apulian foreland. The 'horst and graben' topography of the Murge resulted from Quaternary extensional tectonics associated with the flexural uplift of the Apulian foreland. The top of the Murge ridge separates a northeastern side characterized by a stepped topography that gently dips to the Adriatic Sea, and a karst plateau bounded by a steep tectonic escarpment to the SW (Fig. 3A and C). The southwestern Murge escarpment marks an abrupt transition between the karst plateau and the Ionian coastal plain. Two tectonic escarpments also separate the Murge topography from the Tavoliere di Puglia plain to the NW and the Salento peninsula to the SE (Fig. 3A and B).

The northeastern side of the Murge karst landscape is dissected by a system of shallow, ephemeral streams (locally known as 'lame') discharging into the Adriatic Sea and characterized by narrow valleys and torrential flow regime. The steeper southwestern escarpment of the Murge limestone Plateau is incised by the 'Gravine' streams forming narrow, deep and meandering fluviokarst canyons (Fig. 3B and C). Both drainage systems source in the inner karst landscape, which extends into areas displaying lower and more subdued relief (Fig. 4).

The higher local relief and slopes observed along the southwestern flank of the Murge Plateau suggest higher long-term tectonic uplift and erosion of the Gravine compared with the 'Lame' streams draining the smoother, low-relief topographic surface on the opposite flank (Fig. 4). On the northeastern side of the Murge ridge, local relief and elevations increase to the SE, where the Murge uplands terminate in a prominent, NE-facing fault scarp (the 'Selva di Fasano' escarpment). This steep inland cliff is ~40 km long and separates the easternmost Murge karst Plateau and the coastal plain stretching along the Adriatic coast (Fig. 3C, profile III-III′). Compared with the southwestern Murge escarpment, this area is characterized by the total absence of hydrography across the Selva di Fasano escarpment and a higher concentration of karst features (dolines, poljies, and caves), suggesting that karst dissolution of carbonate rocks is the dominant process.

4.2. Morphometric analysis of drainage basins

We performed a morphometric analysis of 13 'Gravine' basins draining the southwestern escarpment of the Murge Plateau (Table 1). Catchment denudation rates scale with mean local relief (Ahnert, 1970). Interestingly, the 'DB45', 'DB6', and 'DB7' drainage basins include larger plateau areas and exhibit lower mean local relief. We calculated the hypsometric curves and integrals from the basin topography to investigate the equilibrium state of each catchment and the relative dominance of fluvial and hillslope processes along the southwestern escarpment of the Murge Plateau (Fig. 1). The 'DB1', 'DB2', 'DB3','DB4', 'DB6', and 'DB7' drainage basins include large portions of poorly incised surfaces in their upper part, and exhibit steep channels downstream and high *HI* index. The studied drainage basins do not display an inverse correlation between catchment area and *HI* index, suggesting that the hypsometric integral is not an indicator of the relative dominance of hillslope and fluvial processes (Table 1).

Basins 'DB1'–'DB7', located in the western sector (Fig. 5A) display convex hypsometric curves corresponding to higher *HI* values (0.47–0.62), indicating actively uplifting basins. The steep toe in the lower part of these curves suggests instability due to base level fall. The eastern group of basins 'DB8'–'DB13' (Fig. 5B) have hypsometric curves with a more varied shape, from slightly convex ('DB10') to concave ('DB8'), and *HI* values ranging from 0.33 to 0.61. We estimated the Hack's law coefficients (Eq. (1)) for each basin (Table 1). Most of the basins display values of the area exponent, *h*, within the range of 0.5–0.6, and a mean value of 0.53.

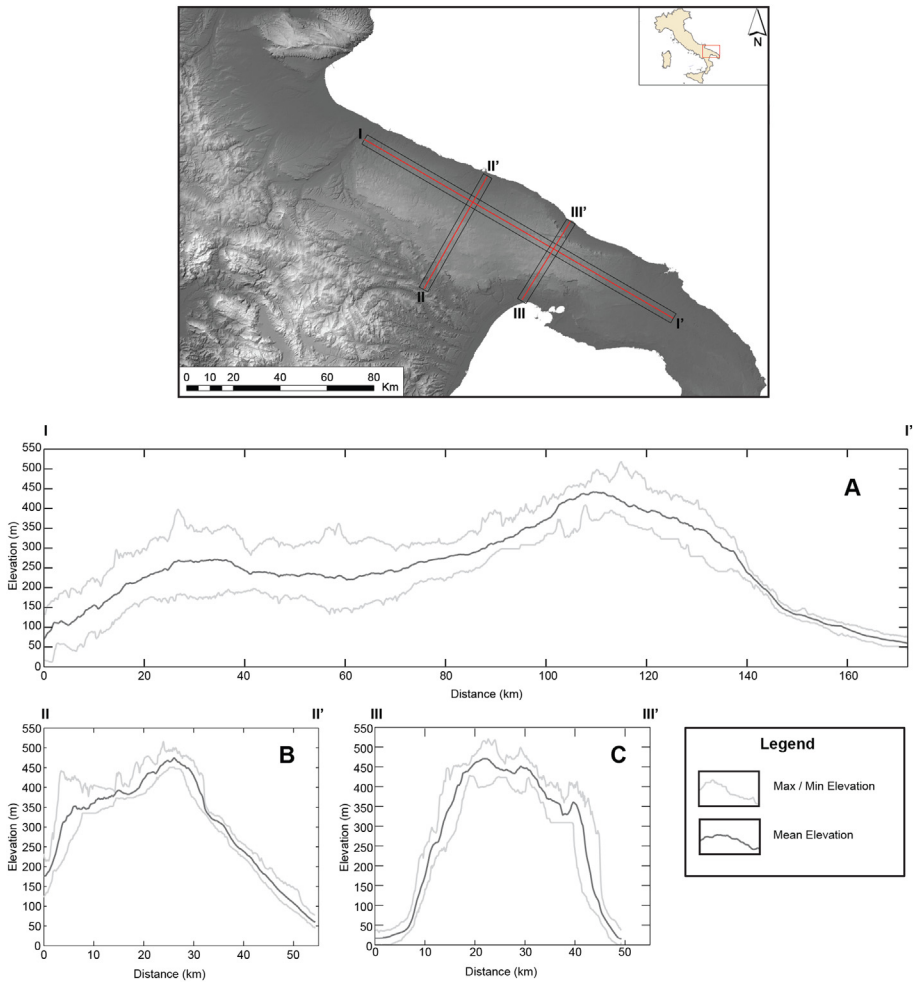

Fig. 3. Topography of Murge area as determined by swath profiles taken along its (A) length (I-I′ profile) and (B, C) width (II-II′ and III-III′ profiles) showing the trend of maximum, mean and minimum heights.

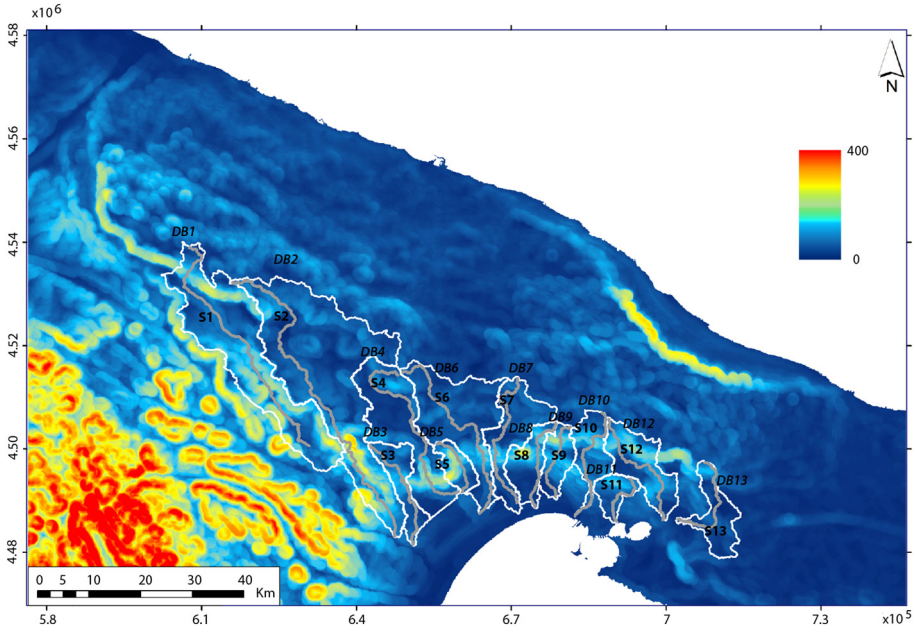

Fig. 4. Map of the local relief of Murge area overlain with the location of the 13 drainage basin DB1-DB13 analyzed in this study (white polygons).

Table 1
mlr = mean local relief in a 500 m window, mlr_{std} = standard deviation of mean local relief, tbr = total relief, HI = drainage basin hypsometric integral, h = Hack's index, c = Hack's coefficient, L = channel length.

Basin name	Basin area (km^2)	mlr (m)	mlr_{std} (m)	tbr (m)	HI	c	h	L (km)
DB1	366.17	65.08	42.68	509	0.62	1.44	0.61	59.93
DB2	602.55	47.16	35.65	609	0.61	1.56	0.59	80.60
DB3	81.39	41.2	20.78	485	0.51	0.60	0.85	29.11
DB4	241.94	36.84	30.26	492	0.62	0.98	0.68	46.75
DB5	36.71	57.58	35.53	385	0.47	0.50	0.91	14.63
DB6	257.38	30.81	18.61	506	0.58	1.72	0.56	47.63
DB7	136.16	31.63	19.88	453	0.62	0.92	0.70	35.8
DB8	83.4	43.68	34.9	453	0.33	2.31	0.51	21.88
DB9	62.44	52.42	30.40	448	0.46	1.82	0.57	18.71
DB10	86.29	45.62	24.33	520	0.61	1.64	0.59	28.71
DB11	34.47	44.50	23.12	272	0.51	1.62	0.54	13.82
DB12	129.82	48.16	31.15	495	0.48	1.62	0.56	29.77
DB13	92.7	22.25	16.55	299	0.40	1.72	0.55	25.69

4.3. River profiles, χ-plot, and steepness map analyses

We extracted 13 longitudinal profiles representing the main trunk channel of each drainage basin (Fig. 6). Only bedrock channel reaches were included in our analyses. In general, the longitudinal profiles display two concave segments separated by a major convex reach (knickpoint). Major knickpoints occur at 200–450 m and in a variety of lithologies. Some river profiles exhibit minor knickpoints that are related to local changes in rock type or normal faults. The upper concave reaches are less steep than the lower ones and correspond to the low relief landscape on the limestone plateau.

The best-fit values of m/n for the 13 basins ranged from −0.39 to 0.55. Most of the basins have a best-fit m/n value below 0.3, suggesting that they are out of equilibrium. The 'DB8' and 'DB13' drainage basins exhibit m/n values of 0.43 and 0.55 and R^2 values of 0.58 and 0.75, respectively, indicating that most of their channels are close to equilibrium.

The k_s value for each basin covaries with the best-fit concavity value (Table 2). Most of the χ-plots display a marked increase of channel steepness below a major knickpoint occurring at 200–450 m, indicating transience due to a change of base-level fall. Minor changes of normalized channel steepness are related to normal faults or lithology changes. The 'S1' and 'S13' streams exhibit near-linear χ-plots, suggesting that these river profiles could be close to equilibrium. We observed that the major knickpoints of the 'S2', 'S4', 'S6' and 'S7' χ-plots are shifted toward lower χ values compared with adjacent streams. To test whether disequilibrium in these river profiles was produced by area capture, we recalculated the χ-plots of the 'DB2', 'DB4', 'DB6', and 'DB7' drainage basins after removing the drainage area of the hypothesized capture from the basin DEM (Fig. 8). The results of the drainage area test show that the χ-plot of the trunk channel collapses toward the trend displayed by the tributaries that were not involved in the area capture.

We used the map of the normalized channel steepness index superimposed on the geological map of the Murge area to distinguish regional trends and local effects related to lithology contrasts. The steep fluviokarst canyons incising the southwestern Murge escarpment have normalized channel steepness $k_{sn} > 60$ $m^{0.9}$ (Fig. 9), suggesting that the underlying limestones represent the most resistant bedrock. However, high anomalies of channel steepness, with k_{sn} values increasing up to >100 $m^{0.9}$, were observed for the 'Gravine' streams draining large portions of the low-relief landscape above the Murge Plateau. In contrast, the k_{sn} of channel segments above the Murge escarpment is generally <20 $m^{0.9}$, suggesting a transient landscape that is equilibrated to a former base level. Minor steepness changes are related to lithology contrasts between the limestone and siliciclastic rocks. Indeed, the values of k_{sn} decrease drastically in the areas below ~200 m, where the transition from the Apulian carbonate to siliciclastic rocks of the Bradanic Trough occurs.

5. Discussion

Our morphometric analysis documented a transient fluvial landscape along the southwestern margin of the Murge Plateau, where prominent knickpoints marked the position of a transient wave of river incision. The presence of preserved low relief surfaces in the uplands and the steep slopes below major knickpoints in the middle reaches of the 'Gravine' trunk channels indicated disequilibrium between uplift and fluvial incision. In addition, most of the major knickpoints displayed similar χ values, suggesting that the transient incision could be related to a recent change of regional base-level. We also found minor knickpoints in the lower and upper catchments corresponding to lithological contrasts and fault traces juxtaposing different lithologies. The convex-shape of the hypsometric curves and high values of the *HI* index calculated for the analyzed drainage basins confirmed that disequilibrium was produced by the active regional uplift since the Middle Pleistocene described by previous studies (Doglioni et al., 1994, 1996; Patacca and Scandone, 2001). Prior research shows the dependence of the hypsometric integral on catchment area: smaller catchments display high hypsometric integrals, indicating dominance of hillslope processes, whereas larger basins dominated by fluvial incision display low hypsometric integrals (Willgoose and Hancock, 1998;

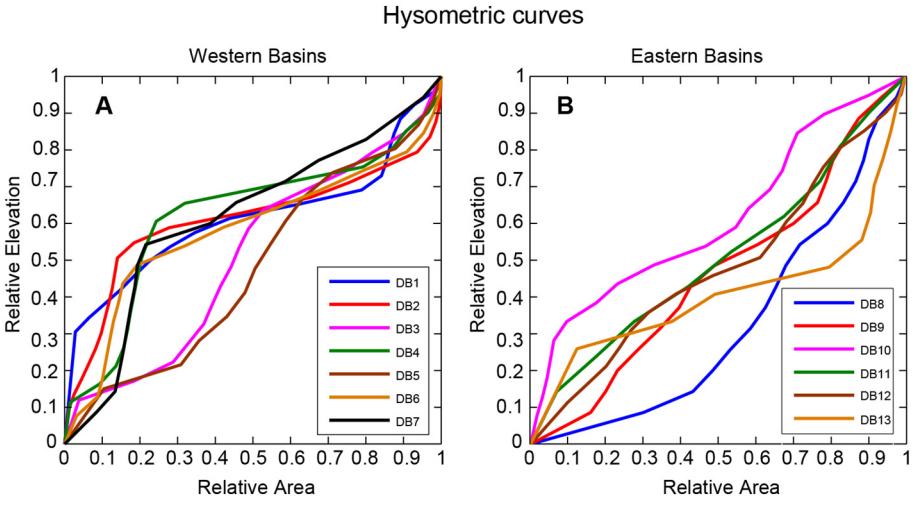

Fig. 5. Hypsometric curves calculated for western (A) and eastern (B) basin draining the southwestern escarpment of the Murge Plateau.

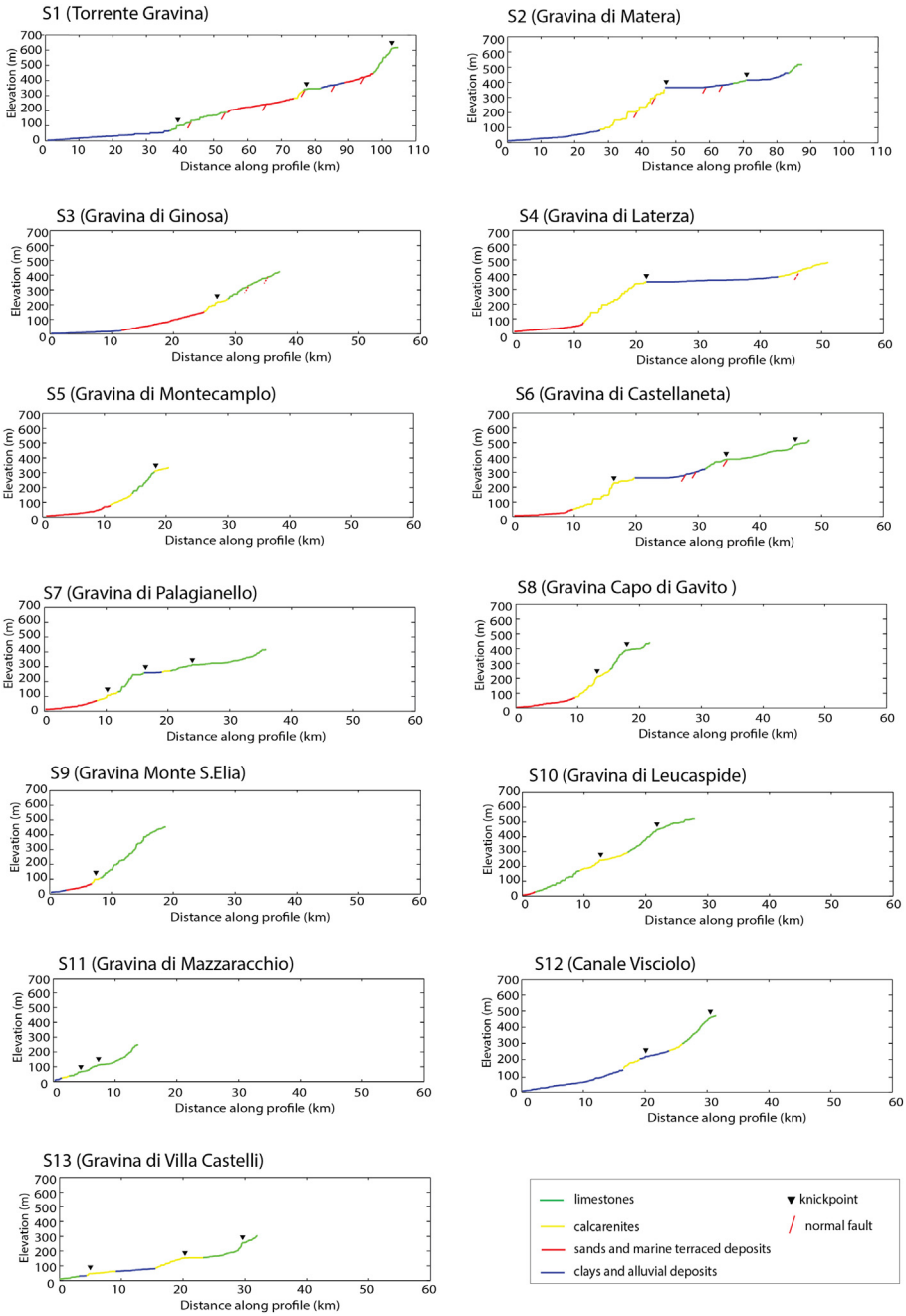

Fig. 6. Trunk channel river profiles for the 13 basins of this study plotted versus outlet. Rock types over which each river flow is shown by different colors. Knickpoints are shown as black triangles.

Table 2
k_s value, R^2 and best-fit m/n values for the 13 basins.

Basin name	Best-fit m/n	R^2	k_s
DB1	0.26	0.87	0.93
DB2	0.05	0.68	0.02
DB3	0.18	0.94	0.32
DB4	−0.39	0.58	8.63×10^{-6}
DB5	0.16	0.81	0.28
DB6	−0.02	0.93	0.074
DB7	−0.02	0.93	8.4×10^{-3}
DB8	0.55	0.56	93.62
DB9	0.22	0.86	0.79
DB10	0.02	0.94	0.025
DB11	0.24	0.88	0.78
DB12	0.19	0.87	0.35
DB13	0.43	0.75	8.28

Hurtrez et al., 1999). However, the inverse correlation between *HI* indexes and drainage areas was not observed in the analyzed drainage basins. The observed hypsometric integrals could be influenced by other factors, such as lithology and tectonics (Lifton and Chase, 1992; Hurtrez et al., 1999).

Our regional analysis revealed an interesting distribution of local relief and normalized channel steepness: the highest values were mostly observed in the northwestern drainage basins of the Murge Plateau escarpment, whereas both local relief and k_{sn} anomalies decreased toward the southeast. The χ-plot analysis revealed also steeper channel reaches in the downstream part of the western 'Gravine' drainage basins, suggesting that an uplift gradient decreasing toward the southeast affected the Murge Plateau. Our results are consistent with uplift rates inferred from the elevations of the 125 ka marine terrace, which indicated a linear gradient of uplift along the Ionian coast

during the Upper-Pleistocene, with a maximum rate of 0.31 mm/year to the northwest, and a minimum rate of 0.11 mm/year to the southeast (Bordoni and Valensise, 1998; Mastronuzzi and Sansò, 2002). Field studies show that knickpoints migrate very slowly when bedrock incision is controlled by plucking (e.g., Brocard et al., 2016). Although we do not have direct measurements of knickpoints retreat rates, the altitude and distance from outlet of major knickpoints in the 'Gravine' drainage basins does not seem to be the result of rapid sea-level changes that occurred during the Quaternary, which reached the lowest sea-level at 120 m below present-day sea level during the last glacial period (e.g., Snyder et al., 2000; Waelbroeck et al., 2002). This suggests that the major knickpoints in the 'Gravine' drainage basins were produced by a single, regional base-level change related to the uplift of the Apulian region after the Middle Pleistocene that has since migrated toward the Murge Plateau interior.

The 'S2', 'S4', 'S6' and 'S7' trunk streams displayed prominent perturbations from the steady-state linear trend and anomalously high steepness values in the middle section of the χ-plot, corresponding to the southwestern Murge Plateau escarpment (Fig. 7). Interestingly, these catchments drain larger plateau areas and are characterized by major knickpoints displaying lower χ values compared with adjacent catchments, suggesting that perturbations from the equilibrium trend were produced by drainage area captures from the Murge Plateau (e.g., Giachetta and Willett, 2018b). The swath profiles revealed two parts of the landscapes displaying marked differences in maximum and minimum elevations, suggesting that the upper parts of these catchments could represent old drainage networks equilibrated to a different base-level that underwent a sudden change of base level, possibly by river capture. We tested the hypothesis of plateau area gain by removing the proposed captured drainage areas from each basin, which

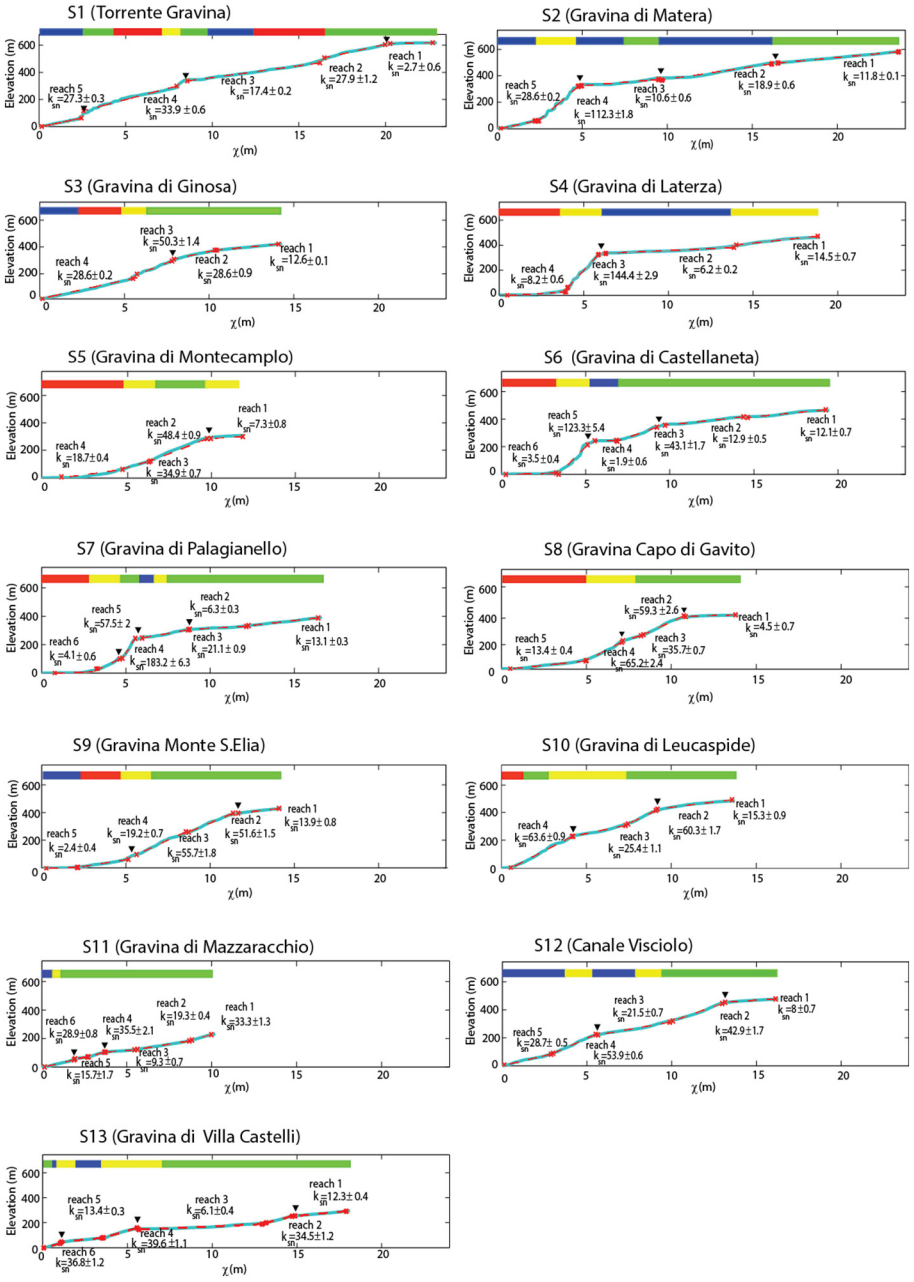

Fig. 7. χ versus elevation plots for analyzed channels (light blue lines). Knickpoints are shown as black triangle and the dashed red lines show the linear regressions used to determine normalized channel steepness index (k_{sn}). Bars show lithologic transitions (see Fig. 6 for legend).

resulted in the trunk channel collapsing above the more linear trend displayed by tributary χ-plots. Our test confirmed that the upper parts of the 'DB2', 'DB4', 'DB6', 'DB7' drainage basins represent old drainage networks or endorheic areas confined above the Murge Plateau that were recently captured from younger escarpment streams by headward erosion. Furthermore, the test revealed colinearity between the trunk and tributaries after the removal of drainage area, suggesting that the m/n value of 0.45 could reflect the steady-state channel concavity for these fluviokarst drainage basins (Giachetta and Willett, 2018b; Francis et al., 2018).

More interestingly, the 'S3' (Gravina di Matera) stream deposited a 20–25 m thick alluvial fan (the 'Parco dei Monaci' alluvial fan; Boenzi, 1954; Boenzi et al., 1976) above the limestone bedrock, where the stream exits the deep fluviokarst canyon and flows across the alluvial plain in the Bradanic Through. The alluvial fan deposit is made of limestone conglomerates and gravels and includes rare limestone boulders with diameter up to 1 m. The 'Parco dei Monaci' alluvial fan possibly records the increased river flow energy and discharge of the 'Gravina di Matera' stream following a large drainage area capture from the Murge Plateau during the Quaternary.

The analysis of the Hack's law suggests that the drainage systems of the 'Gravine' well represent the power scaling between channel length and drainage area observed in fluvial networks (e.g., Hack, 1957; Gray, 1961; Leopold et al., 1964; Mueller, 1972), The obtained values of the Hack's coefficient and exponent confirmed that fluvial development caused by tectonic uplift is the dominant process. The χ-elevation data of reaches underlain by Mesozoic limestones displayed linear channel segments and similar normalized channel steepness values, indicating that the scaling relationships between drainage area, discharge, and channel slope of a standard stream power model hold for the 'Gravine' fluviokarst canyons. The linear fit of limestone channel segments produced the higher channel steepness values suggesting the relatively low influence of chemical weathering on the erodibility of this bedrock type. In addition, we found field evidence that plucking dominates erosion on the jointed limestone bedrock of the Gravine channels (Whipple et al., 2000). Furthermore, the transition from the plateau drainage to the fluviokarst canyons occurs through shallow meandering valleys incised into the Mesozoic limestones, suggesting that incision mainly occurred by surface water flow. These observations, together with the absence of well-developed cave systems in the limestone flanks of the fluviokarst canyons could indicate that the overall evolution of the Gravine streams was dominated by fluvial processes, although we cannot exclude local enhancement of erosion by groundwater sapping during sea-level highstands (e.g., Mastronuzzi and Sansò, 2002). Chemical weathering of carbonate rocks by dissolution was probably more efficient only on the steep valley sides of the Gravine streams and in the highest areas of the Murge Plateau, where abundant dolines were observed in the limestone terrains.

The observed dominance of fluvial landforms in the southwestern Murge Plateau, such as meandering river canyons and valleys, could result from the development of antecedent river valleys over siliciclastic units that overly the Mesozoic limestones (e.g., Boenzi et al., 1976). Allogenic valleys develop on non-karst terrains by concentrated surface flow and carve deep canyons by maintaining their course and water discharge through karst areas (Ford and Williams, 1989; Williams, 2001). Similarly, allogenic river networks developed in the western Murge Plateau by concentrated flow, favored by the impermeable Plio-Pleistocene clay units of the Bradanic Trough and clay-rich 'Terra rossa' soils that cover the limestone bedrock. The onset of regional uplift since the Middle Pleistocene produced the progressive incision of the allogenic valleys into the underlying limestones. Thus, the 'Gravine' canyons are mainly fluvial landforms resulting from vertical incision of antecedent rivers that could maintain their water discharge and keep pace with the regional uplift rate. The stream captures that we identified along the southwestern escarpment of the Murge Plateau were triggered by progressive lowering and headward erosion of the 'Gravine' canyons.

6. Conclusions

The purpose of this study was to investigate the Quaternary landscape evolution of the western Murge Plateau and to characterize the transient state of the 'Gravine' fluviokarst drainage basins. To accomplish these objectives, we performed a morphometric analysis at regional to catchment scale. We extracted morphometric parameters from a 90 m resolution DEM and investigated the equilibrium state of the 'Gravine' trunk channels. Our analysis reveals that the 'Gravine' fluviokarst drainage networks are characterized by well-developed surface drainages, following the typical scaling relationship observed for non-karst bedrock streams.

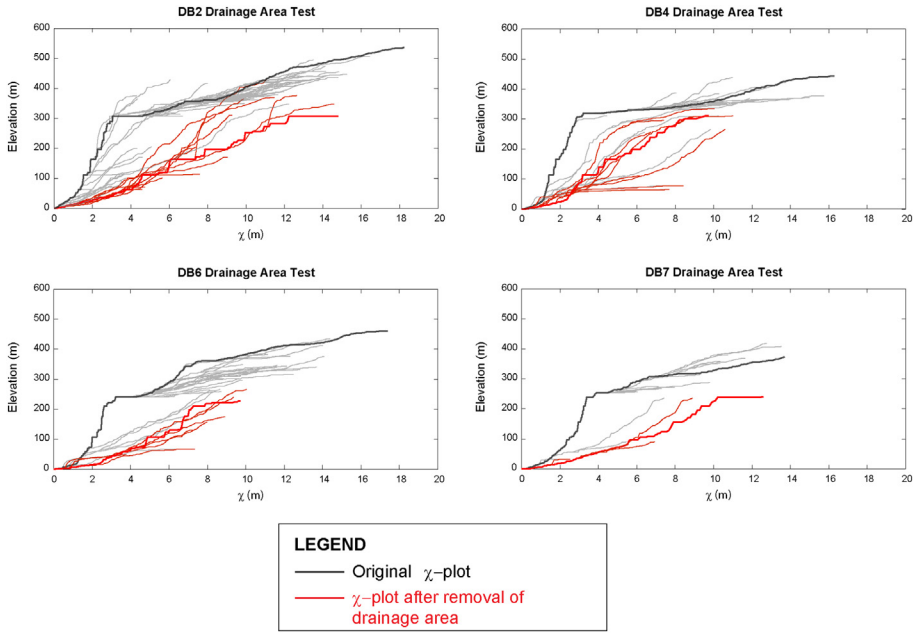

Fig. 8. Drainage area test on catchment affected by capture (DB2, DB4, DB6, DB7).

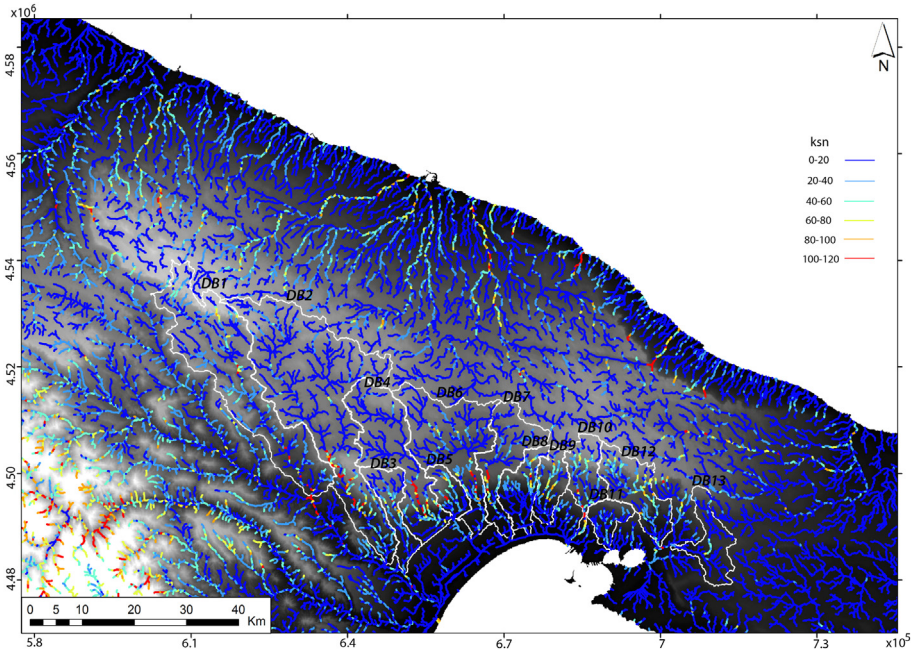

Fig. 9. Map of k_{sn} for the Murge area.

Our results and observations led to the following conclusions:

- the morphometric analysis documents a transient fluvial landscape along the southwestern margin of the Murge Plateau in response to a recent change of regional base-level;
- the convex-shape of the hypsometric curves and high values of the hypsometric integrals calculated for the analyzed basins confirmed that active regional uplift since the Middle Pleistocene produced landscape disequilibrium;
- the regional analysis revealed an interesting distribution of local relief and normalized channel steepness index: the highest values were mostly observed in the northwestern basins along the Murge Plateau escarpment, whereas both local relief and k_{sn} anomalies decreased toward the southeast;
- the χ-plot analysis also revealed steeper channel reaches in the downstream part of the western Gravine basins, suggesting that an uplift gradient with decreasing uplift rates toward the southeast affected the Murge Plateau;
- our analysis highlights the occurrence of major knickpoints displaying lower χ values compared with adjacent catchments. The drainage area test confirmed that perturbations from the equilibrium trend were produced by captures of drainage area from the Murge Plateau, corresponding to the upper parts of these catchments.

Acknowledgements

The authors gratefully acknowledge funding support from the Italian Ministry for Education, Universities and Research (MIUR). We thank two anonymous reviewers and Achim A. Beylich for their constructive reviews and insightful comments that greatly improved the manuscript. The authors are also grateful to Sean F. Gallen for reading, editing, and improving the English text.

References

Ahnert, F., 1970. Functional relationships between denudation, relief, and uplift in large, mid-latitude drainage basins. Am. J. Sci. 268 (3), 243–263.
Amato, A., 2000. Estimating Pleistocene tectonic uplift rates in South-eastern Apenninnes (Italy) from erosional land surfaces and marine terraces. In: Slaymarker, O. (Ed.), Geomorphology. Human Activity and Global Environmental Change. John Wiley & Sons, New York, pp. 67–87.
Anthony, D., Granger, D., 2007. An empirical stream power formulation for knickpoint retreat in Appalachian Plateau fluviokarst. J. Hydrol. 343, 117–126.
Azzaroli, A., Perno, U., Radina, B., 1968a. Note illustrative della Carta Geologica d'Italia, Foglio 188-Gravina di Puglia (Servizio Geologico d'Italia).
Azzaroli, A., Radina, B., Ricchetti, G., Valduga, A., 1968b. Note illustrative della Carta Geologica d'Italia, Foglio 189-Altamura. Servizio Geologico d'Italia 22.
Beneduce, P., Festa, V., Francioso, R., Schiattarella, M., Tropeano, M., 2004. Conflicting drainage patterns in the Matera Horst Area, southern Italy. Phys. Chem. Earth 29 (10), 717–724.
Berlin, M.M., Anderson, R.S., 2007. Modeling of knickpoint retreat on the Roan Plateau, western Colorado. J. Geophys. Res. 112. https://doi.org/10.1029/2006JF00055 F03S06.
Billi, A., 2005. Attributes and influence on fluid flow of fractures in foreland carbonates of southern Italy. J. Struct. Geol. 27 (9), 1630–1643.
Billi, A., Salvini, F., 2003. Development of systematic joints in response to flexure related fibre stress in flexed foreland plates: the Apulian forebulge case history, Italy. J. Geodyn. 36, 523–536.
Bishop, P., Hoey, T.B., Jansen, J.D., Artza, I.L., 2005. Knickpoint recession rate and catchment area: the case of uplifted rivers in Eastern Scotland. Earth Surf. Process. Landf. 30 (6), 767–778. https://doi.org/10.1002/esp.1191.
Boenzi, F., 1954. La Gravina di Matera e i suoi fenomeni di erosione. Rass. Spel. Ital. 31, 123–133.
Boenzi, F., Palmentola, G., Valduca, A., 1971a. Note illustrative della Carta Geologica d'Italia, Foglio 200-Tricarico (Nuova Tecnica Grafica-Roma).
Boenzi, F., Radina, B., Ricchetti, G., Valduga, A., 1971b. Note illustrative della Carta Geologica d'Italia, Foglio 201-Matera. Servizio Geologico Italiano 1–48.
Boenzi, F., Palmentola, G., Valduga, A., 1976. Caratteri geomorfologici dell'area del Foglio "Matera". Bollettino della Società Geologica Italiana 95, 527–566.
Bordoni, P., Valensise, G., 1998. Deformation of the 125 ka marine terrace in Italy: tectonic implications. Geological Society, London. Spec. Publ. 146 (1), 71–110.
Brocard, G.Y., Willenbring, J.K., Miller, T.E., Scatena, F.N., 2016. Relict landscape resistance to dissection by upstream migrating knickpoints. J. Geophys. Res. Earth Surf. 121, 1182–1203. https://doi.org/10.1002/2015JF003678.
Casnedi, R., 1988. La Fossa bradanica: origine, sedimentazione e migrazione. Mem. Soc. Geol. It 41, 439–448.
Ciaranfi, N., Maggiore, M., Pieri, P., Rapisardi, L., Ricchetti, G., Walsh, N., 1979. Considerazioni sulla neotettonica della Fossa bradanica. Progetto Finalizzato Geodinamica del CNR 251, 73–95.
Cucci, L., Cinti, F.R., 1998. Regional uplift and local tectonic deformation recorded by the Quaternary marine terraces on the Ionian coast of northern Calabria (southern Italy). Tectonophysics 292 (1–2), 67–83.
Dai Pra, G., Hearty, P.J., 1988. I livelli marini pleistocenici del Golfo di Taranto. Sintesi geocronostratigrafica e tettonica. Memorie Societa` Geologica Italiana 41, 637–644.
Dai Pra, G., Steams, C.E., 1977. Sul Tirreniano di Taranto: Datazioni su coralli con il metodo del Th^{230}/U^{234}. Geol. Romana 16, 231–242.
D'Argenio, B., 1974. Le piattaforme carbonatiche periadriatriche. Una rassegna di problemi nel quadro geodinamico mesozoico dell'area mediterranea. Memorie della Società Geologica Italiana 13, 137–159.
Delle Rose, M., Parise, M., 2002. Karst subsidence in South-Central Apulia, Southern Italy. Int. J. Speleol. 31, 181–199.
Dewey, J.F., Helman, M.L., Knott, S.D., Turco, E., Hutton, D.H.W., 1989. Kinematics of the western Mediterranean. Geol. Soc. Lond., Spec. Publ. 45 (1), 265–283.

Doglioni, C., Mongelli, F., Pieri, P., 1994. The Puglia uplift (SE-Italy): an anomaly in the foreland of the Apenninic subduction due to buckling of a thick continental lithosphere. Tectonics 13, 1309–1321.
Doglioni, C., Tropeano, M., Mongelli, F., Pieri, P., 1996. Middle-Late Pleistocene uplift of Puglia: an "anomaly" in the Apenninic foreland. Mem. Soc. Geol. Ital. 51, 101–117.
Dunne, T., 1980. Formation and controls of channel networks. Prog. Phys. Geogr. 4 (2), 211–239.
Dunne, T., 1990. Hydrology, mechanics, and geomorphic implications of erosion by subsurface flow. In: Higgins, C.G., Coates, D.R. (Eds), Groundwater Geomorphology: The Role of Subsurface Water in Earth-Surface Processes and Landforms. Geological Society of America Special Paper 252, 1–28.
Favali, P., Funiciello, R., Mattietti, G., Mele, G., Salvini, F., 1993. An active margin across the Adriatic Sea (central Mediterranean Sea). Tectonophysics 219, 109–117.
Ferranti, L., Antonioli, F., Amorosi, A., Dai Prà, G., Mastronuzzi, G., Mauz, B., Monaco, C., Orrù, P., Pappalardo, M., Radtke, U., Renda, P., Romano, P., Sansò, P., Verrubbi, V., 2006. Markers of the last interglacial sea-level high stand along the coast of Italy: tectonic implications. Quat. Int. 145-146, 30–54.
Festa, V., Sabato, L., Tropeano, M., 2018. 1: 5,000 geological map of the upper Cretaceous intraplatform-basin succession in the "Gravina di Matera" canyon (Apulia Carbonate Platform, Basilicata, southern Italy). Ital. J. Geosci. 137 (1), 3–15.
Fielding, E.J., Isacks, B.L., Barazangi, M., Duncan, C., 1994. How flat is Tibet? Geology 22, 163–167.
Flint, J.J., 1974. Stream gradient as a function of order, magnitude, and discharge. Water Resour. Res. 10, 969–973.
Ford, D.C., Williams, P.W., 1989. Karst Geomorphology and Hydrology. vol. 601. Unwin Hyman, London.
Francis, A.K., Peterson, E.W., Dogwiler, T.J., 2018. Lithology as an erosional control on the cave branch and horn hollow fluviokarst watersheds in Carter County, Kentucky. In: Sasowsky, I.D., Byle, M.J., Land, L. (Eds.), 15th Multidisciplinary Conference on Sinkholes and the Engineering and Environmental Impacts of Karst and the 3rd Appalachian Karst Symposium. Shepherdstown vol. 6. West Virginia, National Cave and Karst Research Institute, pp. 279–288.
Frankel, K.L., Pazzaglia, F.J., 2005. Tectonic geomorphology, drainage basin metrics, and active mountain fronts. Geogr. Fis. Din. Quat. 28 (1), 7–21.
Gallen, S.F., Wegmann, K.W., 2017. River profile response to normal fault growth and linkage: an example from the Hellenic forearc of south-central Crete, Greece. Earth Surface Dynamics 5 (1), 161.
Giachetta, E., Willett, S.D., 2018a. A global dataset of river network geometry. Scientific data 5, 180127.
Giachetta, E., Willett, S.D., 2018b. Effects of river capture and sediment flux on the evolution of plateaus: insights from numerical modeling and river profile analysis in the upper Blue Nile catchment. Journal of Geophysical Research: Earth Surface 123 (6), 1187–1217.
Gilbert, G.K., 1877. Report on the Geology of the Henry Mountains. US Government Printing Office.
Gilchrist, A.R., Summerfield, M.A., Cockburn, H.A.P., 1994. Landscape dissection, isostatic uplift, and the morphologic development of orogens. Geology 22, 963–966.
Gray, D.M., 1961. Interrelationships of watershed characteristics. J. Geophys. Res. 66, 1215–1223.
Grohmann, C.H., 2004. Morphometric analysis in geographic information systems: applications of free software GRASS and R. Comput. Geosci. 30 (9–10), 1055–1067 ISSN 0098-3004. https://doi.org/10.1016/j.cageo.2004.08.002.
Hack, J.T., 1957. Studies of longitudinal profiles in Virginia and Maryland. USGS Professional Paper 294-B.
Howard, A.D., 1994. A detachment-limited model of drainage basin evolution. Water Resourses Research 30, 2261–2285.
Howard, A.D., Kerby, G., 1983. Channel changes in badlands. Geol. Soc. Am. Bull. 94 (6), 739–752.
Hurtrez, J.E., Sol, C., Lucazeau, F., 1999. Effect of drainage area on hypsometry from an analysis of small-scale drainage basins in the Siwalik Hills (Central Nepal). Earth Surface Processes and Landforms: The Journal of the British Geomorphological Research Group 24 (9), 799–808.
Iannone, A., Pieri, P., 1982. Caratteri neotettonici delle Murge. Geologia Applicata e Idrogeologia 17, 147–159.
Isacks, B.L., 1992. Long term land surface processes: erosion, tectonics and climate history in mountain belts. In: Mather, P. (Ed.), TERRA-1: Understanding the Terrestrial Environment, pp. 21–36.
Kirby, E., Whipple, K.X., 2012. Expression of active tectonics in erosional landscapes. J. Struct. Geol. 44, 54–75. https://doi.org/10.1016/j.jsg.2012.07.009.
Kirkby, M.J., Chorley, R.J., 1967. Throughflow, overland flow and erosion. Hydrol. Sci. J. 12 (3), 5–21.
Kühni, A., Pfiffner, O.A., 2001. The relief of the Swiss Alps and adjacent areas and its relation to lithology and structure: topographic analysis from a 250-m DEM. Geomorphology 41 (4), 285–307.
Leopold, L.B., Maddock, T., 1953. The Hydraulic Geometry of Stream Channels and some Physiographic Implications. vol. 252. US Government Printing Office.
Leopold, L.B., Wolman, M.G., Miller, J.P., 1964. Fluvial Processes in Geomorphology. 522, Freeman. CA (USA), San Francisco.
Lifton, N.A., Chase, C.G., 1992. Tectonic, climatic and lithologic influences on landscape fractal dimension and hypsometry: implications for landscape evolution in the San Gabriel Mountains, California. Geomorphology 5 (1–2), 77–114.
Mackin, J.H., 1948. Concept of the graded river profile. Geol. Soc. Am. Bull. 59 (5), 463–512.
Manfreda, S., Sole, A., De Costanzo, G., 2015. Le precipitazioni estreme in Basilicata. Universosud Società Cooperativa, Potenza, Italy, p. 146.
Mannella, S., 1977. La gravina di Castellaneta. Mem. Ist. Geogr. Fac. Econ. e Comm. Univ. Bari 7.
Mariotti, G., Doglioni, C., 2000. The dip of the foreland monocline in the Alps and Apennines. Earth Planet. Sci. Lett. 181 (1–2), 191–202.
Martinis, B., Robba, E., 1971. Note illustrative della carta Geologica d'Italia, F 202-Taranto. Boll. Serv. Geol. It, Roma.
Mastronuzzi, G., Sansò, P., 1993. Inquadramento geologico e morfologico della Gravinadi Riggio (Grottaglie,Taranto). Itinerari Speleologici, ser. II 7, 23–36.
Mastronuzzi, G., Sansò, P., 2002. Pleistocene sea-level changes, sapping processes and development of valley networks in the Apulia region (southern Italy). Geomorphology 46, 19–34.
Merla G. and Ercoli A., 1971. Note Illustrative della Carta Geologica d'Italia alla scala 1: 100.000, Foglio 190, Monopoli. Servizio Geologico d'Italia, Roma, Italy.
Mongelli, F., Ricchetti, G., 1970. The earth's crust and heat flow in the Fossa Bradanica, Southern Italy. Tectonophysics 10 (1–3), 103–125.
Montgomery, D.R., Brandon, M.T., 2002. Topographic controls on erosion rates in tectonically active mountain ranges. Earth Planet. Sci. Lett. 201, 481–489.
Montgomery, D.R., Foufoula-Georgiou, E., 1993. Channel network representation using digital elevation models. Water Resour. Res. 29, 1178–1191.
Moresi, M., Mongelli, G., 1988. Underlying limestones and dolostones in Apulia, Italy. Clay Miner. 23, 439–446.
Mueller, J.E., 1972. Re-evaluation of the relationship of master streams and drainage basins. Geol. Soc. Am. Bull. 83, 3471–3474.
Parise, M., 2003. Flood history in the karst environment of Castellana-Grotte (Apulia, southern Italy). Nat. Hazards Earth Syst. Sci. 3 (6), 593–604.
Parise, M., 2006. Geomorphology of the Canale di Pirro karst polje (Apulia, Southern Italy). Z. Geomorphol. Suppl. 147, 143.
Parise, M., 2007. Pericolosità geomorfologica in ambiente carsico: le gravine dell'arco ionico tarantino. Atti e memorie della Commissione grotte "Eugenio Boegan" 41, 81–93.
Patacca, E., Scandone, P., 2001. Late thrust propagation and sedimentary response in the thrust-belt—foredeep system of the Southern Apennines (Pliocene-Pleistocene). Anatomy of an Orogen: The Apennines and Adjacent Mediterranean Basins. Springer, Dordrecht, pp. 401–440.
Perron, J., Royden, L., 2013. An integral approach to bedrock river profile analysis. Earth Surf. Process. Landf. 38, 570–576. https://doi.org/10.1002/esp.3302.
Phillips, J.D., 2017. Landform transitions in a fluviokarst landscape. Z. Geomorphol. 61 (2), 109–122.
Phillips, J.D., 2018. Historical contingency in fluviokarst landscape evolution. Geomorphology 303, 41–52.
Pieri, P., Festa, V., Moretti, M., Tropeano, M., 1997. Quaternary tectonic activity of the Murge area (Apulian Foreland – Southern Italy). Ann. Geofis. 40 (5), 1395–1404.
Ricchetti, G., 1980. Contributo alla conoscenza strutturale della Fossa Bradanica e delle Murge. Bollettino della Società Geologica Italiana 99 (4), 421–430.
Royden, L., Patacca, E., Scandone, P., 1987. Segmentation and configuration of subducted lithosphere in Italy: an important control on thrust-belt and foredeep-basin evolution. Geology 15 (8), 714–717.
Schorghofer, N., Jensen, B., Kudrolli, A., Rothman, D., 2004. Spontaneous channelization in permeable ground: theory, experiment, and observation. J. Fluid Mech. 503, 357–374. https://doi.org/10.1017/S0022112004007931.
Schwanghart, W., Kuhn, N.J., 2010. TopoToolbox: a set of Matlab functions for topographic analysis. Environ. Model Softw. 25 (6), 770–781.
Schwanghart, W., Scherler, D., 2014. TopoToolbox 2 – MATLAB-based software for topographic analysis and modeling in Earth surface sciences. Earth Surface Dynamics 2, 1–7. https://doi.org/10.5194/esurf-2-1-2014.
Scotti, V.N., Molin, P., Faccenna, C., Soligo, M., Casas-Sainz, A., 2014. The influence of surface and tectonic processes on landscape evolution of the Iberian Chain (Spain): quantitative geomorphological analysis and geochronology. Geomorphology 206, 37–57. https://doi.org/10.1016/j.geomorph.2013.09.017.
Snyder, N., Whipple, K.X., Tuker, G.E., Merritts, D.J., 2000. Landscape response to tectonic forcing: digital elevation model analysis of stream profiles in the Mendocino triple junction region, northern California. Geol. Soc. Am. Bull. 112 (8), 1250–1263.
Spalluto, L., Caffau, M., 2010. Stratigraphy of the mid-Cretaceous shallow-water limestones of the Apulia Carbonate Platform (Murge, Apulia, southern Italy). Ital. J. Geosci. 129 (3), 335–352.
Strahler, A.N., 1952. Hypsometric (area-altitude) analysis of erosional topography. Geol. Soc. Am. Bull. 63 (11), 1117–1142.
Telbisz, T., Kovács, G., Székely, B., Szabó, J., 2013. Topographic swath profile analysis: a generalization and sensitivity evaluation of a digital terrain analysis tool. Z. Geomorphol. 57 (4), 485–513.
Tropeano, M., 1992. Aspetti geologici e geomorfologici della Gravina di Matera "Parco Archeologico Storico Naturale delle Chiese Rupestri del Materano". Itinerari Speleologici 2, 19–33.
Tropeano, M., Sabato, L., 2000. Response of Plio-Pleistocene mixed bioclastic-lithoclastic temperate-water carbonate systems to forced regressions: the Calcarenite di Gravina Formation, Puglia, SE Italy. Geological Society of London Spec. Publ. 172 (1), 217–243.
Tropeano, M., Sabato, L., Pieri, P., 2002. Filling and cannibalization of a foredeep: the Bradanic Trough, Southern Italy. Geol. Soc. Lond., Spec. Publ. 191 (1), 55–79.
Tucker, G.E., Slingerland, R., 1997. Drainage basin responses to climate change. Water Resour. Res. 33 (8), 2031–2047.
Valduga, A., 1973. Fossa bradanica. Geologia dell'Italia. UTET 692–695.
Waelbroeck, C., Labeyrie, L., Michel, E., Duplessy, J.C., McManus, J.F., Lambeck, K., Balbon, E., Labracherie, M., 2002. Sea-level and deep water temperature changes derived from benthic foraminifera isotopic records. Quat. Sci. Rev. 21 (1–3), 295–305.

Whipple, K.X., Tucker, G.E., 1999. Dynamics of the stream-power river incision model: implications for height limits of mountain ranges, landscape response timescales, and research needs. J. Geophys. Res. 104 (B8), 17661–17674.
Whipple, K.X., Tucker, G.E., 2002. Implications of sediment-flux-dependent river incision models for landscape evolution. Journal of Geophysical Research: Solid Earth 107 (B2).
Whipple, K.X., Hancock, G.S., Anderson, R.S., 2000. River incision into bedrock: mechanics and relative efficacy of plucking, abrasion, and cavitation. Geol. Soc. Am. Bull. 112, 490–503.
Whittaker, A.C., 2012. How do landscapes record tectonics and climate? Lithosphere 4 (2), 160–164. https://doi.org/10.1130/rf.l003.1.
Willett, S.D., McCoy, S.W., Perron, J.T., Goren, L., Chen, C.Y., 2014. Dynamic reorganization of river basins. Science 343. https://doi.org/10.1126/science.1248765.
Willgoose, G., Hancock, G., 1998. Revisiting the hypsometric curve as an indicator of form and process in transport-limited catchment. Earth Surface Processes and Landforms: The Journal of the British Geomorphological Group 23 (7), 611–623.
Williams, P.W., 2001. Karst and solution processes. In: Sturman, A., Spronken-Smith, R. (Eds.), The physical environment; a New Zealand Perspective. Oxford University Press, New York, pp. 307–325.
Wobus, C., Whipple, K.X., Kirby, E., Snyder, N., Johnson, J., Spyropolou, K., Crosby, B., Sheehan, D., 2006. Tectonics from topography: procedures, promise and pitfalls. In: Willet, S., Hovius, N., Brandon, M.T., Fisher, D.M. (Eds.), Tectonics, Climate, and Landscape Evolution. Geological Society of America. Spec. Pap. 398, 55–74.
Woodside, J., Peterson, E.W., Dogwiler, T., 2015. Longitudinal profile and sediment mobility as geomorphic tools to interpret the history of a fluviokarst stream system. Int. J. Speleol. 44 (2), 8.
Yang, R., Willett, S.D., Goren, L., 2015. In situ low-relief landscape formation as a result of river network disruption. Nature 520, 526–529. https://doi.org/10.1038/nature14354.